J Electroceram
DOI 10.1007/s10832-017-0067-0

Resistive switching characteristics and conducting nanobits of polycrystalline NiO thin films

Yoonho Ahn[1] **· Joonkyung Jang**[2] **· Jong Yeog Son**[1]

Received: 6 July 2016 / Accepted: 11 January 2017

Abstract Thin films of NiO were deposited on Pt/Ta/glass sub-strates using a radio frequency (RF) sputtering method. The NiO thin films showed polycrystalline nature, indicating preferentially (111)-oriented structure. The resistive random access memory (RRAM) capacitor of a Pt/NiO/Pt structure exhibited unipolar switching characteristics and bistable resistivities for 200 repeated switching cycles. Furthermore, RRAM nanobits array was formed on the NiO thin films by applying a bias. The RRAM nanobits had a diameter of approximately 8 nm and were observed via a conducting atomic force microscope (CAFM). The density of the RRAM nanobits array was estimated to be approximately 0.64 Tbit/cm^2.

Keywords NiO · Thin film · Polycrystalline · Resistive random access memory · Atomic force microscope

1 Introduction

Non-volatile random access memory (NVRAM) is an attractive data storage device because it can retain information in the absence of power [1–5]. There are many kinds of NVRAMs including magnetic RAM (MRAM), ferroelectric RAM (FeRAM), phase-change RAM (PRAM), resistive RAM (RRAM) as well as conventional Flash memory [6, 7]. Among these, RRAM technology utilizes two switchable resistance states, a high resistance state (HRS) and a low resistance state (LRS), as a binary code [3, 8, 9]. These two resistance states of RRAM materials are easily switched by applying SET and RESET voltages at RRAM capacitors. The resistive switching phenomena are widely observed in various transition metal oxides such as NiO, TiO_2, $SrTiO_3$, $Pr_{0.7}Ca_{0.3}MnO_3$, Cr-doped $SrZrO_3$, and $BiFeO_3$ [9–15]. In particular, nickel oxide (NiO) has been intensively studied as an RRAM material due to its low operating voltages, fast operation speeds, and reproducible resistive switching characteristics [10, 16–21].

RRAM devices have simple metal/insulator capacitor structure (MIM) consisting of one insulating film and two electrodes [16]. Usually, the fabricated thin film exhibits polycrystalline or epitaxial structure with a thickness of approximately a hundred nanometers [10, 21]. Single crystal wafers such as Si and $SrTiO_3$ are widely used as substrates for depositing electrodes and insulating thin films [22, 23]. However, glass substrates for the formation of RRAM capacitors have seldom been used because glasses have amorphous structures. In this study, we investigate the resistive switching characteristics of NiO thin films grown on a glass substrate with Ta adhesion layer and a Pt bottom electrode. We further demonstrate an NiO RRAM nanobits array via conducting atomic force microscope (CAFM).

2 Experimental

Polycrystalline NiO thin films were deposited on Pt/Ta/glass substrates via radio frequency (RF) sputtering. The Pt/Ta/glass substrates were prepared for the deposition of a NiO thin film using the following processes. To obtain a well-

✉ Yoonho Ahn
yahn@khu.ac.kr

✉ Jong Yeog Son
jyson@khu.ac.kr

[1] Department of Applied Physics, Kyung Hee University, Yongin 446-701, South Korea

[2] Department of Nanoenergy Engineering, Pusan National University, Busan 609-735, South Korea

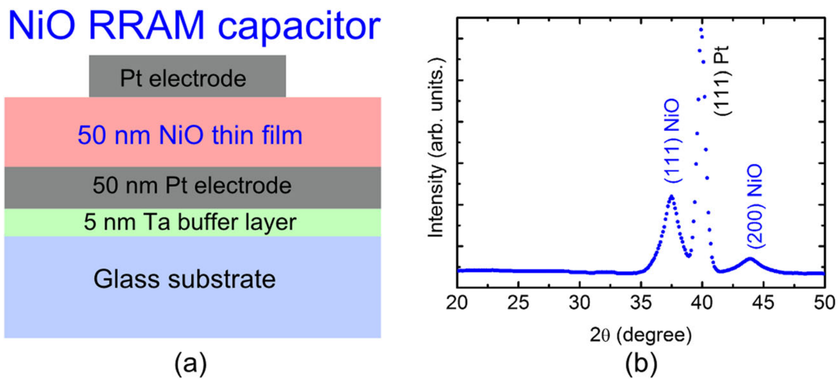

Fig. 1 (**a**) A schematic drawing of the NiO RRAM capacitor made of NiO thin film grown on a Pt/Ta/glass substrate. (**b**) X-ray diffraction pattern of the NiO thin film on the Pt/Ta/glass substrate

crystallized Pt electrode on a glass substrate, a adhesion layer of Ta was deposited between the Pt top electrode and the glass substrate. A 5-nm thick Ta film was deposited as an adhesion layer on glass at 100 W RF power with 10 mTorr Ar gas at 500 °C. After the deposition of the Ta adhesion layer, a 50-nm thick Pt electrode film was deposited on the Ta/glass substrate at 50 W RF power with 10 mTorr at 600 °C. After the preparation of the Pt/Ta/glass substrate, the NiO thin film was fabricated at 100 W RF power with 10 mTorr at 400 °C. The surface morphology and roughness of the NiO thin film were observed via an atomic force microscope (AFM). Figure 1(a) shows a schematic drawing of the NiO RRAM capacitor consisting of two Pt electrodes and one NiO thin film. After the fabrication of the NiO thin film, Pt top electrodes were also prepared using RF sputtering.

3 Results and discussion

First, the structural properties of the NiO thin films on the Pt/Ta/glass substrates were investigated by conducting X-ray diffraction experiments. Figure 1(b) shows the X-ray diffraction (XRD) pattern of the NiO thin film on a Pt/Ta/glass substrate. There are three XRD peaks generated from the Pt bottom electrode and the NiO thin film. The Ta adhesion layer does not exhibit an XRD peak because it is very thin (5 nm in thickness). From the Pt (111) XRD peak, it is inferred that the Pt bottom electrode is preferentially (111)-oriented polycrystalline. In particular, the NiO thin film has two XRD peaks of (111) and (200) orientations, indicating that the NiO thin film is also polycrystalline on the polycrystalline Pt bottom electrode. The full width at half maximums (FWHMs) of the (111) and (200) peaks are broader than that of the Pt bottom electrode, indicating that the NiO thin film has grains smaller than those of the Pt bottom electrode. In addition, the intensity of the (111) XRD peak is significantly larger than that of the (200) XRD peak. Thus, the polycrystalline NiO thin film on the Pt/Ta/glass substrate has preferentially (111)-oriented structure.

To confirm the resistive switching characteristics of the NiO thin film, we examined the current–voltage characteristics in the Pt/NiO/Pt capacitor structure, as shown in Fig. 2(a). The NiO capacitor exhibited a typical unipolar switching behavior. The current values of the R_{ON} and R_{OFF} states are clearly distinguished, indicating that the NiO capacitor has a large resistivity difference between the low resistance state (LRS) and high resistance state (HRS). The SET and RESET voltages, forming the two resistance states of LRS and HRS, were estimated be 1.2 and 2.7 V, respectively. The endurance characteristics of the NiO RRAM capacitors were also investigated to confirm the reliability. The bistable resistances for the HRS and LRS were measured as a function of the

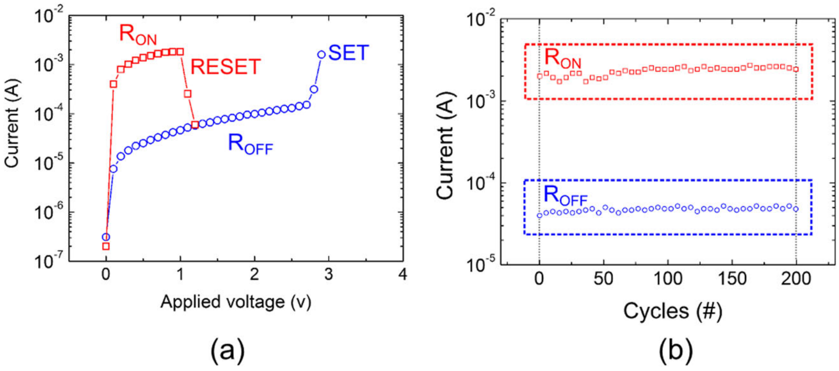

Fig. 2 (**a**) Typical resistive switching characteristics of the NiO RRAM capacitor. (**b**) Bistable resistivities as a function of switching cycle for the NiO RRAM capacitor

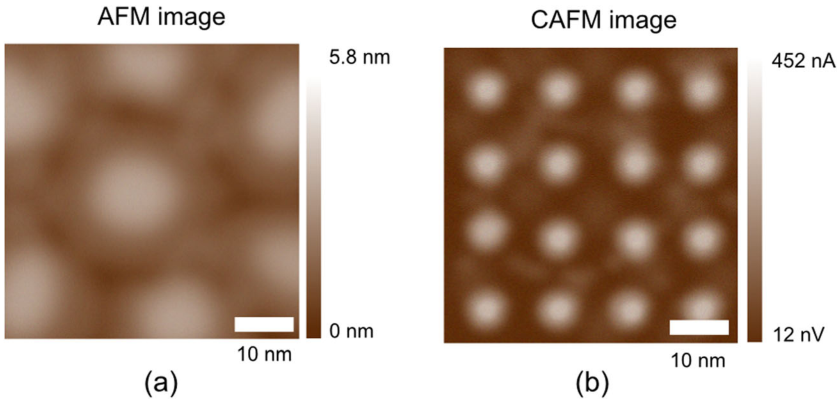

Fig. 3 (**a**) AFM image of the NiO thin film. (**b**) CAFM image of the RRAM nanobit array. The RRAM nanobits have diameters of approximately 9 nm

switching cycle up to 200 (Fig. 2(b)). The endurance and non-overlapping window results reveal that the NiO thin film on glass substrate can potentially be used for memory applications.

To investigate the characteristics of high-density data storage, we demonstrate the formation and observation of RRAM nanobits using CAFM [24, 25]. Figure 3(a) shows an AFM image of the NiO thin film grown on a Pt/Ta/glass substrate. There are round grains on the surface of the NiO thin film with an average grain size of approximately 30 nm. It is possible to form a local nanoscale region consisting of conducting filaments by applying a bias between the CAFM tip and the bottom electrode. As a result, this local region functions as a conducting nanobit, electrically conducting as an LRS state. In this study, this conducting nanobit is referred to as an "RRAM nanobit". The RRAM nanobit in an LRS state could be formed by applying a bias of 3.0 V. This RRAM nanobit is conductive and consists of conducting filaments surrounded by insulating NiO thin film. Therefore, the RRAM nanobit array was directly observed by using the CAFM. Figure 3(b) shows a CAFM image of the RRAM nanobit array. The diameter of the RRAM nanobit is approximately 9 nm. We successfully formed and observed sixteen RRAM nanobits on a square area of 50 nm × 50 nm in size. Hence, a density of the RRAM nanodot array was estimated to be approximately 0.64 Tbit/cm^2.

4 Conclusions

In summary, we deposited NiO/Pt/Ta thin films on a glass substrate to fabricate a polycrystalline NiO thin film RRAM. According to XRD analysis, the (111) preferred orientation was observed on the polycrystalline NiO thin film. The NiO RRAM capacitor exhibited typical unipolar switching behavior with SET and RESET voltages of 1.2 and 2.7 V, respectively. We further investigated high-density data storage characteristics based on CAFM measurements. The RRAM nanobits had diameters of approximately 9 nm and the data storage density was approximately 0.64 Tbit/cm^2.

Acknowledgements This work was supported by the National Research Foundation of Korea (NRF) grant funded by the Korean government (No. 2015R1A2A2A0502795).

References

1. G.I. Meijer, Science **319**, 1625 (2008)
2. J. Doo Seok, T. Reji, R.S. Katiyar, J.F. Scott, H. Kohlstedt, A. Petraru, H. Cheol Seong, Rep. Prog. Phys. **75**, 076502 (2012)
3. F. Pan, C. Chen, Z.-s. Wang, Y.-c. Yang, J. Yang, F. Zeng, Prog. Nat. Sci. **20**, 1 (2010)
4. M.J. Lee, Y. Park, D.S. Suh, E.H. Lee, S. Seo, D.C. Kim, R. Jung, B.S. Kang, S.E. Ahn, C.B. Lee, D.H. Seo, Y.K. Cha, I.K. Yoo, J.S. Kim, B.H. Park, Adv. Mater. **19**, 3919 (2007)
5. R. Waser, M. Aono, Nat. Mater. **6**, 833 (2007)
6. R. Bez, E. Camerlenghi, A. Modelli, A. Visconti, Introduction to flash memory. Proc. IEEE **91**, 489 (2003)
7. J.S. Meena, S.M. Sze, U. Chand, T.-Y. Tseng, Nanoscale Res. Lett. **9**, 526 (2014)
8. J.S. Lee, S. Lee, T.W. Noh, Appl. Phys. Rev. **2**, 031303 (2015)
9. A. Sawa, Mater. Today **11**, 28 (2008)
10. S. Seo, M.J. Lee, D.H. Seo, E.J. Jeoung, D.S. Suh, Y.S. Joung, I.K. Yoo, I.R. Hwang, S.H. Kim, I.S. Byun, J.S. Kim, J.S. Choi, B.H. Park, Appl. Phys. Lett. **85**, 5655 (2004)
11. B.J. Choi, D.S. Jeong, S.K. Kim, C. Rohde, S. Choi, J.H. Oh, H.J. Kim, C.S. Hwang, K. Szot, R. Waser, B. Reichenberg, S. Tiedke, J. Appl. Phys. **98**, 033715 (2005)
12. Y. Watanabe, J.G. Bednorz, A. Bietsch, C. Gerber, D. Widmer, A. Beck, S.J. Wind, Appl. Phys. Lett. **78**, 3738 (2001)
13. A. Asamitsu, Y. Tomioka, H. Kuwahara, Y. Tokura, Nature **388**, 50 (1997)
14. A. Beck, J.G. Bednorz, C. Gerber, C. Rossel, D. Widmer, Appl. Phys. Lett. **77**, 139 (2000)
15. W.H. Kim, J.Y. Son, H.M. Jang, ACS Appl. Mater. Interfaces **6**, 6346 (2014)
16. I. Hwang, M.-J. Lee, G.-H. Buh, J. Bae, J. Choi, J.-S. Kim, S. Hong, Y.S. Kim, I.-S. Byun, S.-W. Lee, S.-E. Ahn, B.S. Kang, S.-O. Kang, B.H. Park, Appl. Phys. Lett. **97**, 052106 (2010)
17. F. Nardi, D. Deleruyelle, S. Spiga, C. Muller, B. Bouteille, D. Ielmini, J. Appl. Phys. **112**, 064310 (2012)
18. S. Long, C. Cagli, D. Ielmini, M. Liu, J. Sune, IEEE Electron Dev. Lett. **32**, 1570 (2011)
19. U. Russo, D. Ielmini, C. Cagli, A.L. Lacaita, S. Spiga, C. Wiemer, M. Perego, M. Fanciulli, IEEE International Electron Devices Meeting, **775**, (2007)
20. D. Choi, C. Soo Kim, Appl. Phys. Lett. **104**, 193507 (2014)

21. S.R. Lee, K. Char, D.C. Kim, R. Jung, S. Seo, X.S. Li, G.S. Park, I.K. Yoo, Appl. Phys. Lett. **91**, 202115 (2007)
22. J. Sullaphen, K. Bogle, X. Cheng, J.M. Gregg, N. Valanoor, Appl. Phys. Lett. **100**, 203115 (2012)
23. J.Y. Son, Y.H. Shin, Appl. Phys. Lett. **92**, 222106 (2008)
24. T. Tybell, P. Paruch, T. Giamarchi, J.M. Triscone, Phys. Rev. Lett. **89**, 976011 (2002)
25. J.Y. Son, C.S. Park, S.K. Kim, Y.H. Shin, J. Appl. Phys. **104**, 064101 (2008)